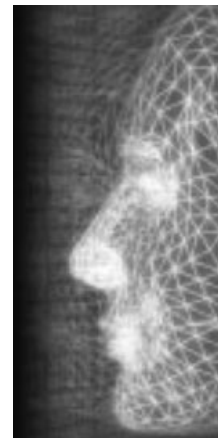


Facial shape and 3D skin

By Won-Sook Lee* and Andrew Soon



We present novel ideas for facial shape and skin simulation on extremely detailed three-dimensional facial meshes. Our input database is composed of a small number of scanned human faces with resolutions up to several million triangles, where even the pores are clearly distinguished. We show how to decompose the facial meshes into the global shape of the face plus skin detail (3D skin), and then to reconstitute them. Our modeling methodology allows us to simulate the exaggeration of the facial global shape, retaining the original skin detail, as well as to transfer 3D skin from one face to another. First, we represent all the input faces in terms of a homogeneous structure on the base model in low resolution by using mesh adaptation techniques. Second, the differences between the original mesh and a base mesh, which appear as skin detail, are captured and stored, so that each face is decomposed into the global shape (a base mesh) plus skin detail. Face reconstitution after global shape exaggeration and/or skin transfer enables delicate simulation of facial models. In addition, we can increase the resolution of any model scanned at a low resolution by transferring skin from a higher resolution model. Our method shows successful manipulation of the minute structure of 3D skin differently from other methods such as Normal Mapping, Displacement Mapping, Displaced Subdivision Surfaces, and Normal Meshes where none of these techniques show manipulation of minute structure like ours and only approximation is used while our method recovers the original structure. Copyright © 2006 John Wiley & Sons, Ltd.

Received: 10 April 2006; Revised: 2 May 2006; Accepted: 10 May 2006

KEY WORDS: 3D skin; exaggeration; skin transfer; mesh adaptation; generic model; Global shape

Introduction

Skin is a naturally-furnished garment for all of us; the skin accounts for about 16% of the body weight,¹ has a typical surface area of 1.5 to 2.0 m² in adults and has a thickness from 0.2 mm (eye lids) to 6.0 mm (sole of foot). Apart from covering the face and body, it also provides clues as to a person's age, health, condition, etc. Even though skin is a very salient topic in everyday life (exemplified by widespread cosmetics use and the

pervasive advertising of such products), skin research in the area of computer graphics has been mainly limited to 2D texture, consisting only of flat (2D) information represented by color, reflectance, and absorption characteristics for photo-realism, even though true skin has a 3D structure that is fine-scale, complicated, and delicate. Some 3D biomechanical simulations² have been performed on skin without visualization of realistic 3D structure. This limitation is attributable to equipment incapable of capturing minute skin detail. However, recent progress in scanning equipment³ has made it possible to obtain scans of human faces that have extremely high polygonal counts (10 million triangles) suitable for production use in full-length feature films such as "The Matrix Reloaded."⁴ The geometry in this production was based on a 100-micron resolution scan of plaster cast molds of the actors' faces.

Figure 1(a) shows our database containing a number of scanned human faces with extremely high polygonal counts and Figure 1(b) shows Person A's raw geometry (i.e., no texture image is applied to the model) in which

*Correspondence to: W. Lee, School of Information Technology and Engineering (SITE), University of Ottawa, 800 King Edward Avenue, P.O. Box 450, Stn A, Ottawa, Ontario, Canada K1N 6N5. E-mail: wslee@uottawa.ca

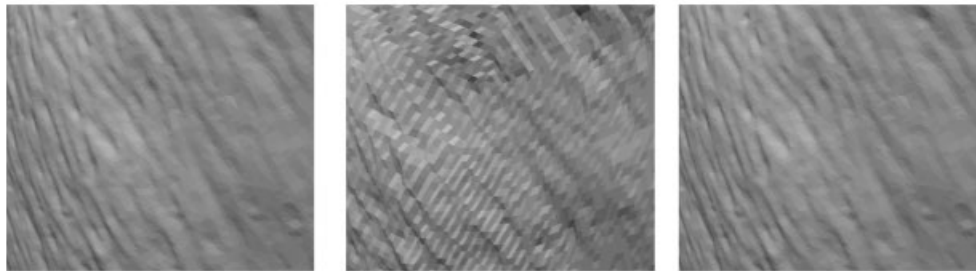
Contract/grant sponsor: Materials and Manufacturing Ontario grant; contract/grant number: IA90193.

Contract/grant sponsor: University of Ottawa Initiation of Research/New Direction Funding; contract/grant number: 103268.

Contract/grant sponsor: Natural Sciences and Engineering Research Council of Canada DISCOVERY; contract/grant number: RGPIN-298691-2004.

Person A	Person B	Person C	Person D	Person E
				
~1.0 M triangles	~2.2 M triangles	~30 K triangles	~3.0 M triangles	~1.5 M triangles

(a)



(b)

(c)

(d)

Figure 1. (a) Our face database; (b)–(d) Magnified view of the left side of Person A's; (b) Original scanned face model. (c) Reconstructed model obtained using displacement mapping; (d) Reconstructed model obtained using our methods.

the 3D structure of human skin can be seen. In this paper, we focus on the skin detail (referred to as 3D skin) as well as the global shape of the 3D facial mesh. We aim to change the appearance of scanned faces by means of shape exaggeration and skin detail transfer. We also investigate the topic of adding 3D skin detail to a model whose resolution is insufficient to yield realistic skin representation. The central contributions of this paper to the fields are: (i) the introduction of 3D skin, (ii) the successful separation of global shape and 3D skin from an extremely dense point set, (iii) the successful reconstitution of any global shape and 3D skin, (iv) the exaggeration of extremely detailed 3D facial meshes of arbitrary resolutions, and (v) the transfer of 3D skin to the base model of a low resolution scanned model in order to increase said scanned model's resolution.

Exaggeration

Exaggeration is one of the key animation principles,⁵ making output more attractive and distinctive by exaggerating the shape, color, emotion, or actions of a character. Many studies have been conducted into the use of exaggeration in digital works. However, a 3D

facial-caricaturing algorithm^{6,7} is usually applied on morphable models (with approximately 70 K triangles) to exaggerate the distinctive information. As the faces in our database have an extremely high-level of detail (up to several million triangles) and they are not morphable, our proposed exaggeration method is considered to be more general.

Transfer From One to Another

In 3D face research for computer graphics and animation, transfer generally refers to motion transfer. There have been many methods developed mainly for mapping performances of one individual to the facial/body animations of another or for transferring global shape/texture of one person to another.^{8–13} Alternating faces in real life has become a hot topic recently, after the world's first face transplant was performed at the end of 2005. The result of a computer-simulated face transplant¹ produced using forensic

¹Hayes L, McAvoy J. Transcript: new faces. Interview for 60 Minutes 2003. Accessed online on 2006 May 5 at http://sixtyminutes/stories/2003_05_18/story_850.asp.

anthropology software is shown on a website², but the process and algorithms are not publicly available. In this paper, we do not aim for medically sound transplant simulation, but for a way to swap face skin details to achieve a similar effect.

Dense Data Manipulation & Structure Embedding

A common approach to avoid the computational expense, inefficiency and even intractability inherent in treating a very dense data set is to first perform the desired changes on a low polygon approximation of the original model and then use advanced techniques such as detail recovery. Normal Mapping^{14,15} is a render-time technique used to create the illusion of detail on a surface. The major disadvantage of normal mapping is that there are no physical changes to the geometry of the rendered surface. Displacement Mapping¹⁶ is a well-known technique used in computer graphics to augment the appearance of a surface. Displacement mapping yields a more detailed surface by perturbing a base surface along its normal. However, our experiment showed displacement mapping's limitation in producing an extremely detailed minute structure like 3D skin. A displacement mapping result is shown in Figure 1(c) compared to the result using our methods shown in Figure 1(d). Detailed analysis of displacement mapping can be found in our previous literature.¹⁷ Lee *et al.*¹⁸ proposed an efficient representation of high resolution geometry called displaced subdivision surfaces (DSS) which essentially represents the high resolution detail as a scalar displacement field over a smooth domain surface. The DSS representation is constructed in three steps: building a base model, optimizing the base model, and generating the displacement map. Normal Meshes¹⁹ are another way to represent surfaces using only a single value per vertex as opposed to the traditional three per vertex, that is, a floating point value for each coordinate of 3-space. The multi-resolution nature of normal meshes also makes it suitable for a wide range of applications. Both DSS and normal meshes are approximate; these representations may not be able to represent very finely detailed surfaces (e.g., human skin) even with a very large number of levels. Additionally, the original structure of the surface cannot be recovered by either representation.

²<http://www.sciencemuseum.org.uk/antenna/facetransplant/>

Mesh adaptation (mesh refinement or consistent mesh parameterization), in simple terms, refers to adaptation of an initial mesh to accurately capture features²²⁻²⁴ and it can provide a useful base to determine the locations of landmarks such as the eyes and nose for every subject; consequently, automatic exaggeration of features by using a homogenous (morphable) structure is feasible. Mesh adaptation on a scanned model makes use of a generic model to govern identified feature information as well as the structure of every face at any resolution. We adapt a generic mesh to the scanned surface, focusing on high quality shape approximation.

Proposed Methodology Outline

A low polygon approximation of a highly detailed model is prepared by employing two-step mesh adaptation (one with feature points and the other with surface refinement) with all low polygon models sharing the same structure. Our procedure captures the skin detail (3D skin) of the original scanned face by performing model parameterization. Parameterization is achieved by mapping the points of a scanned face onto its low polygon approximation and allows the high resolution model to be reconstructed from the low resolution model. A caricature algorithm, which employs a center model (an average model of all the low polygon models) for the purpose of comparison, is applied to the low polygon models. The resulting exaggerated model and the 3D skin drive a reconstruction (recomposition) process that produces an exaggerated model which preserves the accurate detail in the original scanned face. The shared structure of low polygon models and 3D skin also permits the transfer of skin detail from one to another.

Homogeneous Structure Embedding

This section describes how we embed a desired homogeneous structure of a generic model on several scanned faces with various face sizes and various resolutions.

Our five scanned face models of differing resolutions shown in Figure 1(a) are presented with closed eyes and mouth due to the use of plaster modeling in the scanning process. Person C has the entire head region available,

but the model has only 30K triangles whereas other scanned faces lack the region at the back of the head including the ears, but have very high resolutions. The generic model with 1485 triangles has efficient triangulation, with finer triangles over the highly curved or highly articulated regions of the face and larger triangles elsewhere as shown in Figure 2(a). In addition, the eyes and mouth of the generic model are closed since our scanned models' eyes and mouth were always closed.

point correspondence between the generic model and the scanned model in order to deform the generic model using radial basis function (RBF) networks.^{25,26} Correspondence requires feature points to be located on 2D visualizations of the scanned face. With interactively chosen front view features, the side view feature locations are calculated automatically by finding the depth on the scanned model input. More details can be found in our previous work.¹⁷ Figure 2(b) shows the feature-based model M_F obtained using feature information and RBF.

Feature-Based Model Construction

The basic idea is to let feature locations on a scanned face lead the deformation of the generic model toward individualization. Several approaches have been developed.^{11,22,23} We semi-automatically establish 3D feature

Global Shape Construction

Loop's subdivision scheme,^{18,27} designed to achieve a smooth surface, is applied once to the feature-based model to increase the number of triangles. The resulting

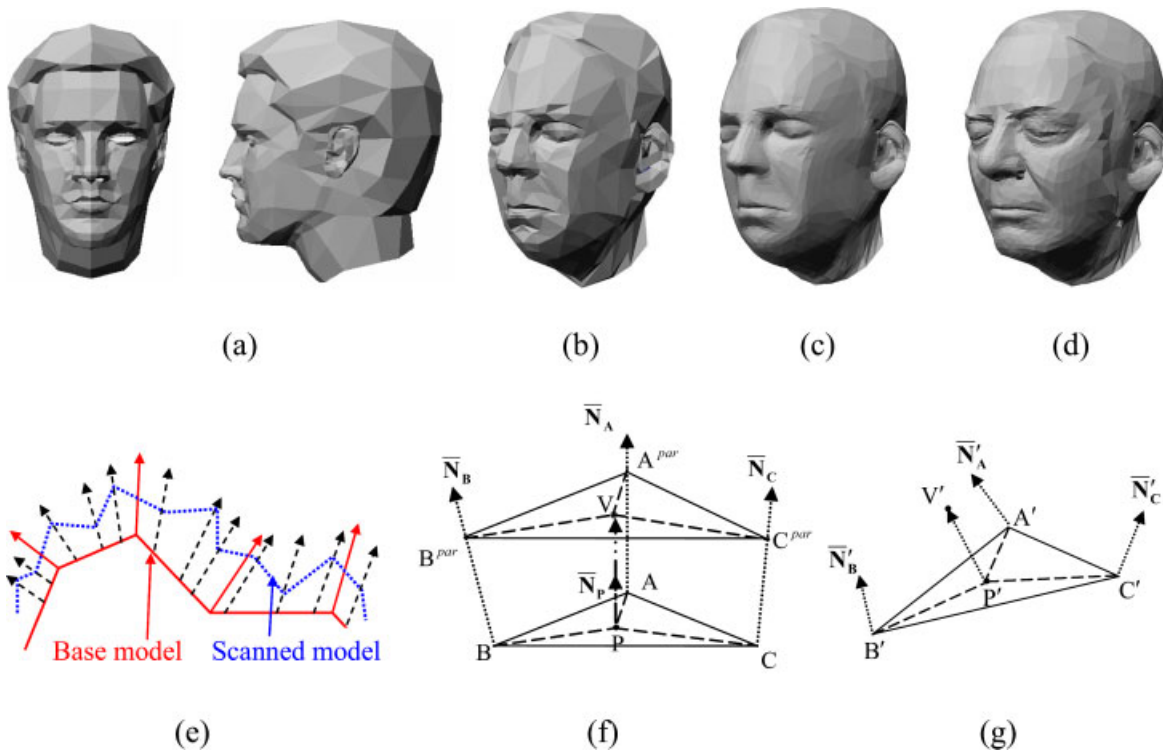


Figure 2. Global shape and detail (3D Skin) construction: (a) Generic model (1.5 K triangles); (b) Feature-based model of Person A (1.5 K triangles); (c) Feature-based model subdivided once (6 K triangles); (d) Base model obtained after model refinement (6 K triangles); (e) 2D version of point-to-surface mapping. A corresponding point on the base model is found for each point of the detailed original scanned model; (f) Example of point-to-surface mapping where point V is mapped to ΔABC . $\Delta A^{par}B^{par}C^{par}$ and ΔABC lie on parallel planes and $A^{par}, B^{par}, C^{par}$ and V are all coplanar; (g) Reconstruction of a point V following the displacement of ΔABC to $\Delta A'B'C'$. Its new position is denoted by V' .

model, consisting of about 6K triangles as shown in Figure 2(c), is then subjected to model refinement to bring its appearance closer to that of the scanned model. From our experiments, we found the proper resolution and close shape approximation of the low resolution model is crucial for satisfactory detail capture. We refer to the refinement result (i.e., the refined subdivided feature-based model) as the base model M_L , which is of low resolution compared to the original scanned model. The base model serves as the representation of the scanned model's global shape.

While our previous work¹⁷ adopted a ray-casting projection method for shape adaptation, we found that cylindrical projection provides more robust projection. Cylindrical projection can be approximated to a global projection method; as all the projection vectors are based on the axis of the cylinder and their directions are regular. Thus, the projection result does not become affected by very complex and irregular local shape. The images in Figure 2 contrast a feature-based model in (b) and (c) and its corresponding base model in (d). The base model shows high quality approximation of its corresponding scanned model (Person A) in our database. Since the most extremely high resolution scanned models provided to us capture only the face region of the subjects, we remove the back of the head and the ears of each low resolution and use the cropped face area for the following work.

3D Skin Construction

The second component which results from the decomposition of the scanned model is its detail representation D_{O-L} . D_{O-L} is considered to be the difference between the original scanned model and its derivative base model. We term this detail representation 3D skin. We utilize point-to-surface mapping^{20,21} to construct the detail representation. Point-to-surface mapping enables a point in 3D space to be mapped to a surface using 3D ray-casting projection based on interpolated surface normals. The 2D version of this mapping scheme is illustrated in Figure 2(e) in which one interpolated surface normal (referred to as a ray) of the base model is shown passing through each vertex of a scanned model. The origin of the ray then defines a point on the base model to which the corresponding scanned model vertex is mapped.

Figure 2(f) shows the case where a vertex V belonging to a scanned model is mapped to the triangle ABC belonging to the corresponding base model. The

ray origin P and the interpolated vertex normal \bar{N}_P are given by

$$P = (1 - u - v)A + uB + vC$$

$$\bar{N}_P = (1 - u - v)\bar{N}_A + u\bar{N}_B + v\bar{N}_C \quad (1)$$

where u and v are the 2D barycentric coordinates of P with respect to ΔABC . \bar{N}_A , \bar{N}_B and \bar{N}_C are the vertex normals at A, B, and C, respectively. For all points lying within or along the edges of ΔABC , the constraints $u, v \in [0, 1]$ and $u+v \leq 1$ are satisfied. The position of V can then be expressed as

$$V = P + d \frac{\bar{N}_P}{\|\bar{N}_P\|} \quad (2)$$

where d is the signed distance from P to V in the direction of \bar{N}_P and $\|\cdot\|$ denotes vector magnitude. To calculate the values of u and v in Equation (1), a new triangle $A^{par} B^{par} C^{par}$ that is parallel to ΔABC and whose vertices are coplanar with V is defined. The vertices of this new triangle are obtained by finding the intersection of \bar{N}_A , \bar{N}_B and \bar{N}_C with the parallel plane. Computing the barycentric coordinates of V with respect to $\Delta A^{par} B^{par} C^{par}$ yields the values of u and v . In other words,

$$V = (1 - u - v)A^{par} + uB^{par} + vC^{par} \quad (3)$$

The parameterization of an original scanned model is constructed with respect to its corresponding low resolution base model using the aforementioned point-to-surface mapping scheme. This parameterization is achieved by obtaining a set of mapping parameters (l, u, v, d) for each vertex in the original scanned model, where l is an identifier for the base model triangle and u , v , and d are as defined in Equation (1). Parameterization permits the base model's shape to influence the shape of the detailed model since the positions of vertices are affected by changes to the base model's vertex normals (Figure 2(g)). Note, then, that 3D skin is essentially the result of model parameterization.

A two-step process is required to find triangle ABC for each scanned model vertex V . The first step consists of accumulating a 'bin' of scanned model vertices for each low resolution triangle. Only scanned model vertices in the vicinity of a triangle are added to its bin. 'Vicinity' is a function of the bounding box of the triangle and a user-definable tolerance. Bins are not mutually exclusive so that multiple triangles are checked for each vertex. Once the bins have been populated, the point-to-surface scheme is performed iteratively for each vertex-triangle pair and the best set of mapping parameters is chosen for

each scanned model vertex. As the iterative process progresses, each newly calculated parameter set for a particular scanned model vertex is compared to the incumbent set (if one has been established) for the same vertex. The incumbent set is the best set of mapping parameters encountered at any given point in the iterative process and there is at most one incumbent per vertex. A sequence of heuristics is used to decide whether the new set should become the new incumbent. Some of these heuristics include satisfying constraints

for barycentric coordinates, minimizing the value of displacement and minimizing reconstruction error. After all vertex-triangle pairs are checked, the incumbent set for each vertex is used in the scanned model's parameterization.

If there is no incumbent for a vertex, that vertex has no mapping parameters in the model parameterization and, therefore, cannot be reconstructed. This produces a hole in the reconstructed model caused by removing all polygons adjacent to the vertex. Recon-

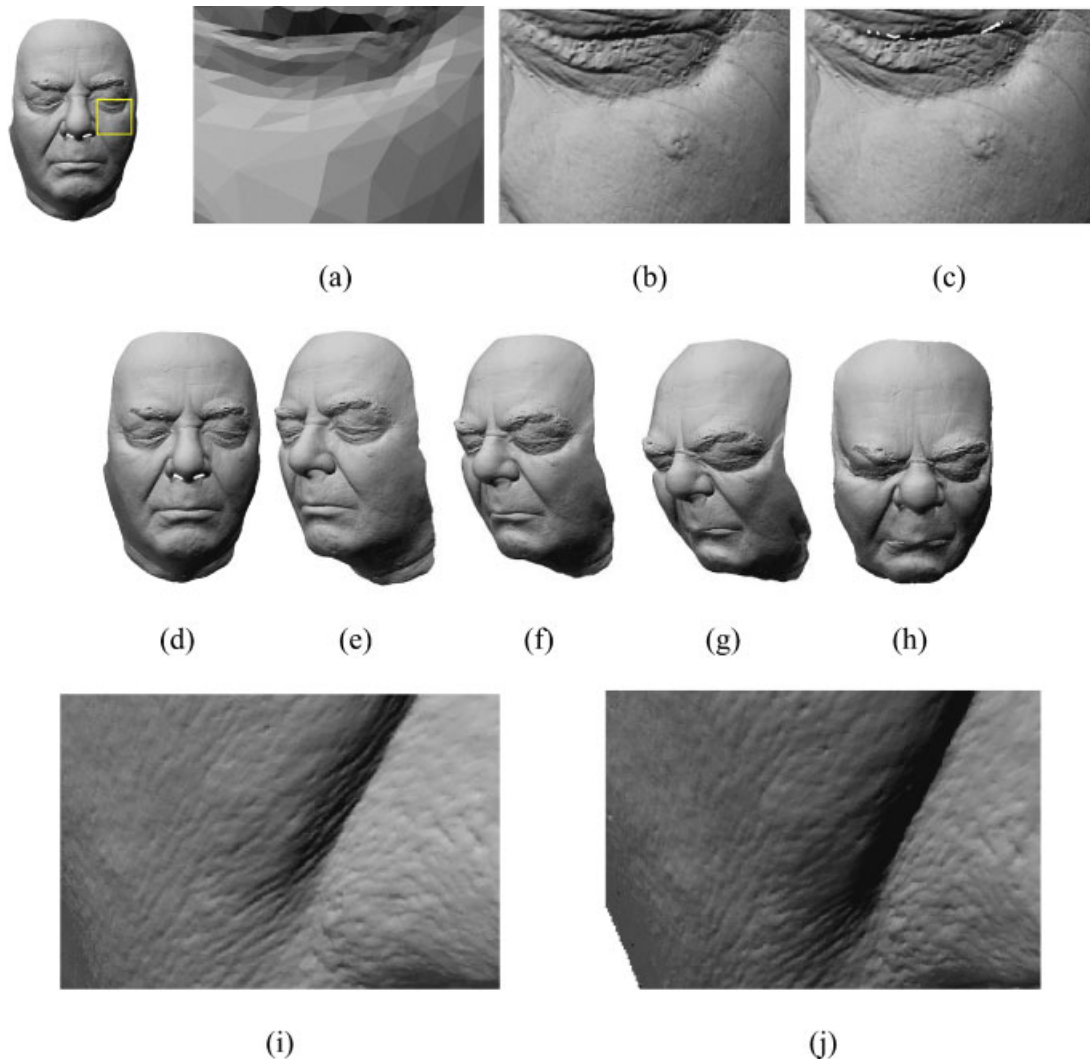


Figure 3. Detail Recovery and comparison: (a) Low resolution model (5900 triangles); (b) Original scanned model (997 025 triangles); (c) Detail-recovered model (937 761 triangles) before filling holes; (d)–(e) Original scanned model; (f)–(h) Exaggerated models obtained using two factors; (f) 60%; (g)–(h) 120%; (i)–(j) Comparison of level of detail; (i) Original scanned model; (j) Detail-recovered model obtained using an exaggeration factor of 75%.

struction is covered in the discussion about detail recovery.

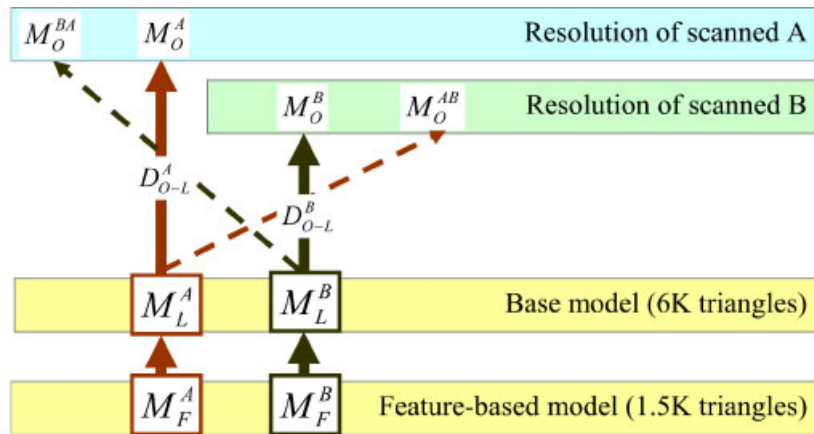
second is skin detail alternation (3D skin transfer) between different scanned faces.

Shape and Detail Simulation

Figure 4(a) shows the decomposition of a scanned model M_O (30K to 3M triangles depending on the scanned resolution) into a feature-based model M_F (1485 triangles), a low resolution base model M_L (5940 triangles), and a skin detail representation D_{O-L} (3D skin). We discuss two kinds of facial simulation applications in this section. The first application is global shape exaggeration and the

Global Shape Exaggeration Through Base Model Exaggeration

Our approach decouples the scanned models' global shape (base model with morphable structure inherited from the generic model) and detail information so that exaggeration is performed only on the global shape and then the detail of the original scanned model is added to



(a)



(b)

Figure 4. (a) Diagram of detail transfer between two base models; (b) Skin detail transfer examples. Left to right: Person A with Person B's skin; Person B with Person A's skin; the original model of Person D; Person D's skin applied on his own 60% exaggerated global shape model; Person A's skin transferred onto Person D's 60% exaggerated global shape model.

return to the original scanned resolution. The idea for the base model exaggeration is to get a center (or average) face and perform vector-based scaling to emphasize the difference between the center and an individual. An exaggerated model $M_L^{\text{exaggeratedPerson}}$ can then be obtained by scaling each feature vector by a constant factor ef as

$$M_L^{\text{exaggeratedPerson}} = M_L^{\text{person}} + ef(M_L^{\text{person}} - M_L^{\text{center}})$$

where M_L^{person} is the base model and M_L^{center} is the center face.

Detail Recovery

The premise of the detail recovery algorithm is to use the model parameterization (3D skin) to reproduce the vertices of the original scanned model. This detail recovery is used on any base model such as the subject's unmodified base model, exaggerated base model, or another subject's base model. The vertex normals are recalculated to reflect the curvature change from the original base model to the new (e.g., exaggerated) base model. Equations (1) and (2) can then be restated as

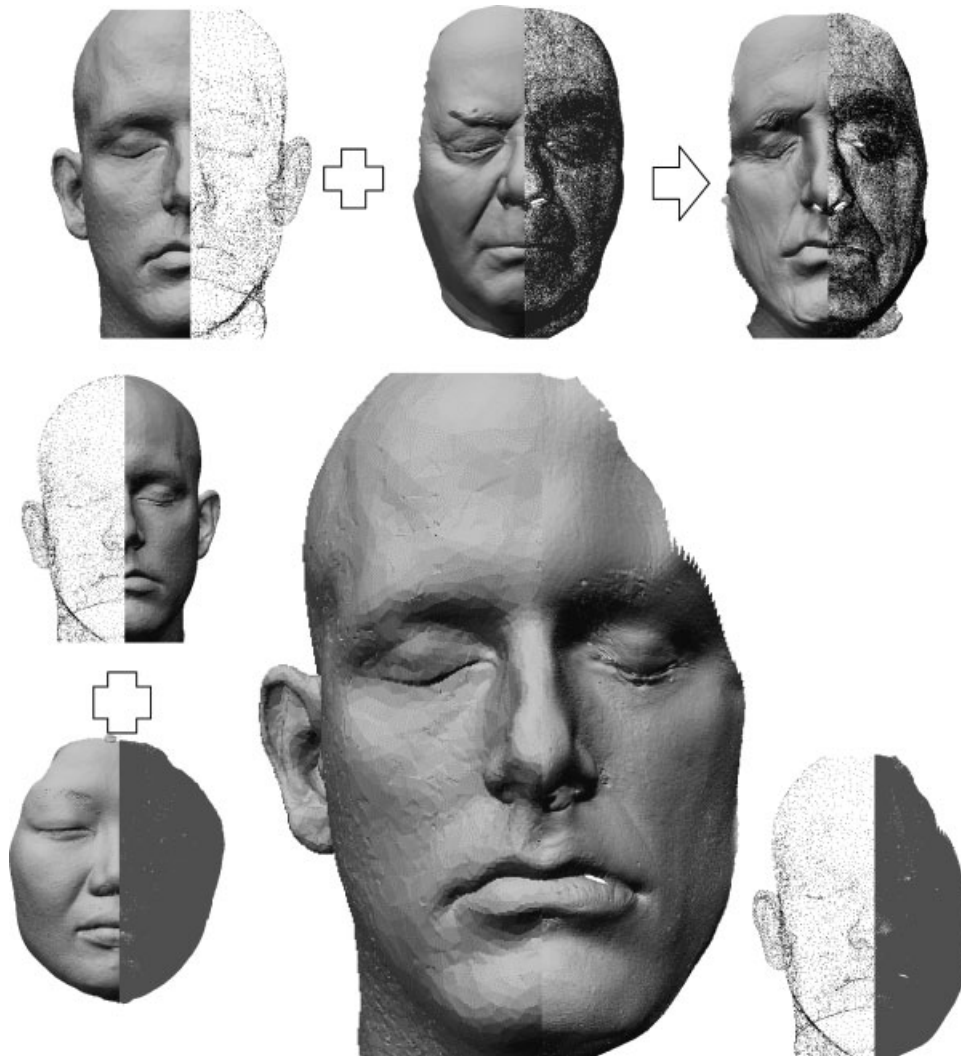


Figure 5. Resolution augmentation through skin detail transfer. Upper row: Transferring Person A's skin detail to Person C (60% shape-exaggerated). Lower row: Transferring Person D's skin detail to Person C (unexaggerated). The center image shows one side of the original face and the opposite side of the new face, illustrating the resolution increase.

$$P' = (1 - u - v)A' + uB' + vC'$$

$$\bar{N}'_{P'} = (1 - u - v)\bar{N}'_A + u\bar{N}'_B + v\bar{N}'_C \quad (4)$$

and

$$V' = P' + d \frac{\bar{N}'_{P'}}{|\bar{N}'_{P'}|}, \quad (5)$$

respectively; the result is illustrated in Figure 2(g). Each set of mapping parameters is applied to the new

state of the base model to reconstruct each detailed model vertex. The detail recovery can be written as

$$M_{LO}^{\text{exaggeratedPerson}} = M_L^{\text{exaggeratedPerson}} + D_{O-L}^{\text{Person}}$$

where the notation + is loosely used here. The number of sets of mapping parameters (I, μ, ν, v) contained in D_{O-L}^{Person} is at most equal to the number of vertices in the original scanned model.

Figure 3(a)–(c) shows a close-up comparison (for Person A) of the base model, the original scanned model, and the detail-recovered model formed from the

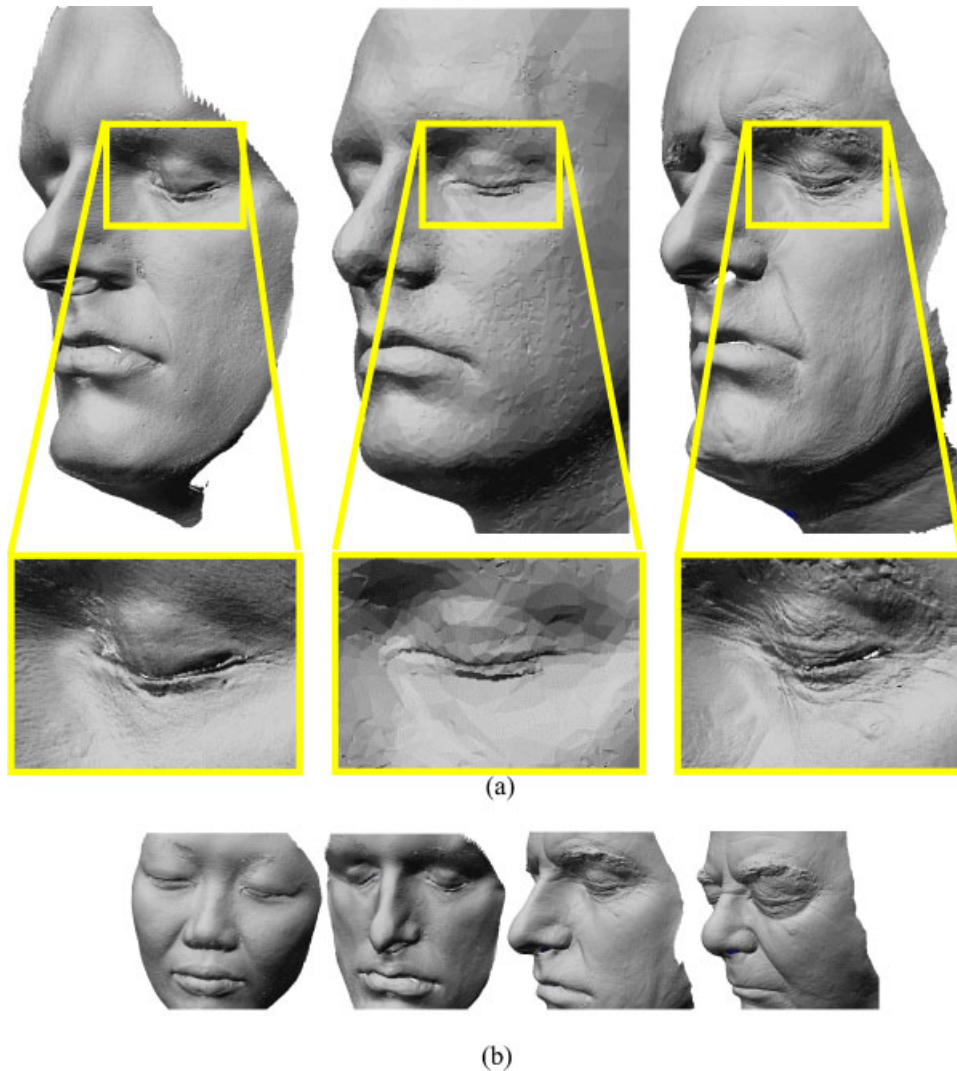


Figure 6. (a) Left to right: Person E's skin detail transferred to 60% shape-exaggerated Person C; original scanned model of Person C; Person A's skin detail transferred to 60% shape-exaggerated Person C. (b) Left to right: Original scanned model of Person E; Person E's skin detail transferred to 60% shape-exaggerated Person C; Person A's skin detail transferred to 60% shape-exaggerated Person C; Original scanned model of Person A.

unmodified base model, respectively. The detail recovered model shows several tiny holes around the eye where scanned model vertices could not be mapped to the base surface. This is due to the very complicated structure in this region resulting in missing intersections within the user-defined threshold to find ΔABC where the information of missing points can be used to remove tiny holes automatically

Some of our results for global shape exaggeration are shown in Figure 3(d)–(h). The images present the results of exaggerating a 1M triangle scanned model at 60% and 120%. The results show the stronger emphasis of the person's facial shape characteristics with a higher exaggeration factor applied. The detail recovery is calculated between the 6K triangle base model and the 1M triangle model of Person A. Figure 3 (i) and (j) shows the close-up comparison of the area to the left of the cheek between the original scanned face and the detail recovered exaggerated models with an exaggeration factor of 75%. The folding becomes deeper on the exaggerated face and the detail is preserved as they are on the original model.

Detail Alternation or 3D Skin Transfer

Our mesh adaptation using the generic model allows us to swap the base models of different people for detail recovery. It is then possible to alternate the skin details (3D skins) between two different human subjects, say Person A and Person B. The original scanned model for Person A can be loosely written as

$$M_O^A = M_L^A + D_{O-L}^A.$$

We can alternate the details between different people, for example, Person A's low resolution shape with Person B's detail. The formula is as follows:

$$M_O^{AB} = M_L^A + D_{O-L}^B.$$

The method used for the exchange of details between two scanned models is shown in Figure 4(a) with dotted lines, including the final resolution after the detail has been transferred. With the decomposition of scanned faces into global shapes and details, any face can be both exaggerated in its global shape and used in conjunction with another person's detail for detail recovery. Figure 4(b) shows the results of skin exchange between Person A and Person B as well as the recovery of Person A's 3D skin on Person D's exaggerated shape.

Resolution Increase of Scanned Model

Another interesting example of exaggeration and skin transfer is shown in Figures 5 and 6 where Person C's unexaggerated or 60% exaggerated shape receives the 3D skin of: (i) Person A (senior Caucasian male), and (ii) Person E (young Asian female). One thing to emphasize here is that the scanned resolution of Person C is only about 30000 triangles, which is insufficient for skin detail representation. However, skin detail transfer allows us to transfer the details from other higher resolution scanned faces so that each resulting detail-recovered face shares the same point distribution as its respective 3D skin donor. Figure 6(a) also shows close-up views of the models' skin details.

Conclusion

This paper presents methodologies used to decompose a scanned face model into global shape and detail (3D skin) and to recompose shape and 3D skin to reproduce the scanned model. A homogeneously-structured representation of a scanned face's global shape (base model) is obtained using two steps of mesh adaptation: (i) feature-driven individualization of a generic model, and (ii) mesh refinement by cylindrical projection. The 3D skin representation of the scanned face can then be calculated by parameterizing the scanned face with respect to the base model, which amounts to mapping the scanned model's vertices onto the base model's triangles. We demonstrate the usefulness of this practice by performing two kinds of facial simulation: (i) detail-preserving shape exaggeration, and (ii) 3D skin (skin detail) transfer. In the latter, the homogeneous structure present in all base models allows the global shape of one person to be recomposed with the 3D skin of a different person, yielding a new model which (i) is at the resolution of the latter's scanned model, (ii) bears the global shape of the former person, and (iii) has the skin detail of the latter person's scanned face. Of particular interest is the case in which the 3D skin originates from an extremely high resolution model while the shape is extracted from a lower resolution model. In this instance, a byproduct of 3D skin transfer is an increase in the resolution of the lower resolution scanned face.

The results of our simulations demonstrate that with the proposed decomposition, we can efficiently control the shape and detail of extremely high-detail scanned data without losing the original resolution. The

computation time is negligible as it takes only a few seconds on a computer using $2 \times$ Opteron 252@2.6 GHz with 4GB of physical memory to perform all the processing as our low resolution model has only 6K triangles.

The scanned models used for this paper possess high-quality approximations of real life skin detail. The second and fifth images in Figure 4(b) and the right-most image in Figure 6(a) show the skin detail of Person A applied onto the base models of Person B, Person D, and Person C (with some exaggeration added). The skin transfer results show the identity is governed by the model whose global shape is used. However, clues as to the person's age, health, condition, etc. arise from the model whose 3D skin is used (here, Person A).

The potential of 3D is large and many innovative facial simulations are possible. Our future research is focused on automatic base model animation through the use of an animation structure in the generic model.

References

1. Lanir Y. Skin mechanics. In *Handbook of Bioengineering*, Skalak R, Chien S (eds). McGraw Hill Book Company: New York, 1987; 11.1–11.25.
2. Magnenat-Thalmann N, Kalra P, L ev eque JL, Bazin R, Batisse D, Querleux B. A computational skin model: fold and wrinkle formation. *IEEE Transactions on Information Technology in Biomedicine* 2002; 6 (4): 317–323.
3. Taylor J, Beraldin J-A, Godin G, Cournoyer L, Rioux M, Domey J. NRC 3D imaging technology for museums & heritage. *Proceedings of The First International Workshop on 3D Virtual Heritage* 2002:: 70–75.
4. Borshukov G, Lewis JP. Realistic human face rendering for "The Matrix Reloaded". *Proceedings of ACM SIGGRAPH 2003 Conference on Sketches & Applications* 2003: 1–1. DOI: 10.1145/965400.965470.
5. Lasseter J. Principles of traditional animation applied to 3D computer animation. *Proceedings of ACM SIGGRAPH 87 (Computer Graphics, 21:4)* 1987: 35–44. DOI: 10.1145/37401.37407.
6. O'Toole AJ, Vetter T, Volz H, Salter EM. Three-dimensional caricatures of human heads: distinctiveness and the perception of facial age. *Perception* 1997; 26: 719–732.
7. Blanz V, Vetter T. A morphable model for the synthesis of 3D faces. *Proceedings of ACM SIGGRAPH 99* 1999: 187–194. DOI: 10.1145/311535.311556.
8. Noh J-Y, Neumann U. Expression cloning. *Proceedings of ACM SIGGRAPH 2001* 2001: 277–288. DOI: 10.1145/383259.383290.
9. Vlastic D, Brand M, Pfister H, Popovic J. Face transfer with multilinear models. *Proceedings of ACM SIGGRAPH 2005* 2005: 223–231. DOI: 10.1145/1073204.1073209.
10. Sumner RW, Popovic J. Deformation transfer for triangle meshes. *ACM Transactions on Graphics (TOG)* 2004; 23 (3): 399–405. DOI: 10.1145/1015706.1015736.
11. Allen B, Curless B, Popovi c Z. The space of human body shapes: reconstruction and parameterization from range scans. *ACM Transactions on Graphics* 2003; 22 (3): 587–594. DOI: 10.1145/882262.882311.
12. K ahler K, Haber J, Yamauchi H, Seidel H-P. Head shop: generating animated head models with anatomical structure. *Proceedings of the 2002 ACM SIGGRAPH Symposium on Computer Animation* 2002: 55–64. DOI: 10.1145/545261.545271.
13. Na K, Jung M-R. Hierarchical retargetting of fine facial motions. *Computer Graphics Forum* 2004; 23 (3): 667–695.
14. Blinn JF. Simulation of wrinkled surfaces. *Proceedings of ACM SIGGRAPH 78* 1978: 286–292. DOI: 10.1145/800248.507101.
15. Peercy M, Airey J, Cabral B. Efficient bump mapping hardware. *Proceedings of ACM SIGGRAPH 97* 1997: 303–306. DOI: 10.1145/258734.258873.
16. Cook RL. Shade trees. *Proceedings of ACM SIGGRAPH 84* 1984: 223–231. DOI: 10.1145/800031.808602.
17. Soon A, Lee W-S. Shape-based detail-preserving exaggeration of extremely accurate 3D faces. Accepted for publication in *The Visual Computer* 2006.
18. Lee A, Moreton H, Hoppe H. Displaced subdivision surfaces. *Proceedings of ACM SIGGRAPH 2000* 2000: 85–94. DOI: 10.1145/344779.344829.
19. Guskov I, Vidimce K, Sweldens W, Schroder O. Normal meshes. *Proceedings of ACM SIGGRAPH 2000* 2000: 95–102. DOI: 10.1145/344779.344831.
20. Sun W, Hilton A, Smith R, Illingworth J. Layered animation of captured data. *The Visual Computer* 2001; 17 (8): 457–474.
21. Hilton A, Starck J, Collins G. From 3d shape capture to animated models. *Proceedings of IEEE Conference on 3D Data Processing, Visualization Transmission* 2002: 246–255.
22. Lee Y, Terzopoulos D, Waters K. Realistic modeling for facial animation. *Proceedings of ACM SIGGRAPH 95* 1995: 55–62. DOI: 10.1145/218380.218407.
23. Lee W-S, Magnenat-Thalmann N. Fast head modeling for animation. *Image and Vision Computing* 2000; 18 (4): 355–364.
24. Praun E, Sweldens W, Schr oder P. Consistent mesh parameterizations. *Proceedings of ACM SIGGRAPH 2001* 2001: 179–184. DOI: 10.1145/383259.383277.
25. Bui TD, Poel M, Heylen D, Nijholt A. Automatic face morphing for transferring facial animation. *Proceedings of 6th IASTED International Conference on Computers, Graphics and Imaging* 2003: 19–23.
26. Noh J-Y, Fidaeo D, Neumann U. Animated deformations with radial basis functions. *Proceedings of ACM Symposium on Virtual Reality Software and Technology* 2000: 166–174.
27. Loop C. Smooth subdivision surfaces based on triangles. Master's thesis, University of Utah, Department of Mathematics, 1987.

Authors' biographies:



Won-Sook Lee is an Assistant Professor at SITE, Faculty of Engineering, University of Ottawa, Canada. She has studied and worked in companies and universities in South Korea, UK, Singapore, Switzerland and U.S.A. She holds a Ph.D. in Computer Science from University of Geneva, Master's degrees from University of Geneva, National University of Singapore and Pohang University of Science and Technology (POSTECH) in Information Systems, Systems Science and Mathematics, respectively, and a B.Sc. in Mathematics from POSTECH. Her main research area is Computer Animation covering topics ranging from Computer Graphics to

Computer Vision, but the main theme is VISUALIZATION and HUMAN.



Andrew Soon holds a B. Eng. in Computer Systems Engineering from Carleton University (Ottawa, Canada) and is currently an M.A.Sc. Electrical Engineering student in the Department of Systems and Computer Engineering at Carleton University. He is also a member of the DISCOVER Lab in the School of Information Technology and Engineering at the University of Ottawa. His research is in the area of 3D face modeling, but is also interested in other topics closely related to video games and computer-generated work for films. These include computer graphics, computer animation, and 3D rendering.